PORTLAND PRESS

## Research Article

# Protein CoAlation: a redox-regulated protein modification by coenzyme A in mammalian cells

Yugo Tsuchiya[1], Sew Yeu Peak-Chew[2], Clare Newell[1], Sheritta Miller-Aidoo[1], Sriyash Mangal[1,3], Alexander Zhyvoloup[1], Jovana Baković[1], Oksana Malanchuk[4], Gonçalo C. Pereira[5], Vassilios Kotiadis[5], Gyorgy Szabadkai[5], Michael R. Duchen[5], Mark Campbell[6], Sergio Rodriguez Cuenca[6], Antonio Vidal-Puig[6], Andrew M. James[7], Michael P. Murphy[7], Valeriy Filonenko[4], Mark Skehel[2] and Ivan Gout[1,4]

[1]Department of Structural and Molecular Biology, University College London, London WC1E 6BT, U.K.; [2]Biological Mass Spectrometry & Proteomics Cell Biology, MRC Laboratory of Molecular Biology, Cambridge CB2 0QH, U.K.; [3]Department of Biology II, Ludwig-Maximilians-Universität München, Planegg-Martinsried 82152, Germany; [4]Institute of Molecular Biology and Genetics, National Academy of Sciences of Ukraine, Kyiv 03680, Ukraine; [5]Department of Cell and Developmental Biology, University College London, London WC1E 6BT, U.K.; [6]Wellcome Trust–MRC Institute of Metabolic Science and MRC Metabolic Diseases Unit, Addenbrooke's Hospital, Cambridge CB2 0QQ, U.K.; and [7]MRC Mitochondrial Biology Unit, Wellcome Trust, MRC Building, University of Cambridge, Cambridge CB2 0XY, U.K.

Correspondence: Ivan Gout (i.gout@ucl.ac.uk)

OPEN ACCESS

Coenzyme A (CoA) is an obligatory cofactor in all branches of life. CoA and its derivatives are involved in major metabolic pathways, allosteric interactions and the regulation of gene expression. Abnormal biosynthesis and homeostasis of CoA and its derivatives have been associated with various human pathologies, including cancer, diabetes and neurodegeneration. Using an anti-CoA monoclonal antibody and mass spectrometry, we identified a wide range of cellular proteins which are modified by covalent attachment of CoA to cysteine thiols (CoAlation). We show that protein CoAlation is a reversible post-translational modification that is induced in mammalian cells and tissues by oxidising agents and metabolic stress. Many key cellular enzymes were found to be CoAlated *in vitro* and *in vivo* in ways that modified their activities. Our study reveals that protein CoAlation is a widespread post-translational modification which may play an important role in redox regulation under physiological and pathophysiological conditions.

## Introduction

Coenzyme A (CoA) is a ubiquitous and essential cellular cofactor synthesised from cysteine, pantothenate (Vitamin B5) and ATP in a pathway conserved in all cells. CoA functions as a master acyl group carrier and a carbonyl-activating group, resulting in numerous metabolically active thioester derivatives, including acetyl CoA, malonyl CoA, succinyl CoA and 3-hydroxy-3-methylglutaryl CoA, among many others. CoA and its derivatives play important roles in a diverse range of cellular processes, including the Krebs cycle, the synthesis and oxidation of fatty acids, ketogenesis, biosynthesis of cholesterol and acetylcholine, regulation of gene expression and cellular metabolism via protein acetylation and others [1–4]. The size of the CoA pool (CoA and all its derivatives) varies widely among mammalian cells and tissues, being largest in the liver, heart and kidney. The subcellular distribution of the CoA pool reflects its diverse roles and varies from 20–140 $\mu$M in the cytosol to 2.2–5 mM in the mitochondria [1]. The level of CoA and the ratio between CoA and its thioesters (acyl CoA) in mammalian cells and tissues are tightly regulated by extracellular stimuli, nutrients, intracellular metabolites and stresses. Insulin, glucose, fatty acids and pyruvate all decrease CoA biosynthesis, whereas fasting, glucagon, glucocorticoids and hypolipidaemic drugs have the opposite effect [5–9]. Changes in the size of the CoA pool have also been reported in pathological conditions, such as diabetes and cancer [10,11]. Mutations in pantothenate kinase 2 (*PANK2*) and CoA synthase (*CoASY*), which are rate-limiting enzymes in the CoA biosynthetic pathway, are associated with a severe

neurodegenerative disorder called NBIA (Neurodegeneration with Brain Iron Accumulation), suggesting that CoA biosynthesis and homeostasis play a crucial role in maintaining the functional integrity of the central nervous system [12,13].

Cysteine plays critical roles in protein structure and function by forming inter- and intra-molecular disulphide bonds, by co-ordinating metal ions and by participating in catalytic reactions. Protein cysteines are targets for post-translational modifications, including S-acylation, oxidation, S-nitrosation, persulfhydration and S-thiolation [14,15]. During oxidative stress, the thiol group of cysteine residues can be progressively oxidised to sulphenic, sulphinic or sulphonic states. The latter two modifications are generally considered to be irreversible and can lead to the loss of protein function. Alternatively, protein cysteines can form mixed disulphides with low-molecular-weight thiols such as glutathione (GSH) by S-thiolation. Glutathionylation is the most studied form of S-thiolation in mammalian cells, which is thought to protect reactive cysteines from irreversible oxidation [16,17]. Additionally, glutathionylation can modulate catalytic activity, regulatory interactions, subcellular localisation and protein stability, thereby playing a key role in redox signalling and the antioxidant defence [18].

The nucleophilic thiol of CoA also participates in thiol-disulphide exchange reactions. CoA disulphides or mixed disulphides with other low-molecular-weight thiols, such as CoA-cysteine and CoA-GSH, have been identified in prokaryotic and eukaryotic cells [19]. The formation of mixed disulphides between CoA and cysteines of specific proteins has been reported in several biochemical and crystallographic studies [20–22]. For example, acetyl-CoA acetyltransferase and glutamate dehydrogenase were found to be covalently bound to CoA in rat liver mitochondria [23], and a CoA-modified form of a peroxide sensor OhrR was detected in *Bacillus subtilis* [21]. However, the extent of covalent protein modification by CoA in prokaryotes or eukaryotes, the induction by oxidative and metabolic stress, and the mechanism of regulation have not been reported.

# Experimental

## Reagents and chemicals

The generation of the anti-CoA antibody (1F10) was described recently [24]. All common chemicals were obtained from Sigma–Aldrich unless otherwise stated. The following antibodies and dilutions were used: mouse anti-CoA antibody (0.17 μg/ml); rabbit anti-actin antibody (Cell Signaling Technology #4968, 1:2000); rabbit anti-tubulin antibody (Cell Signaling Technology #2148, 1:2000); rabbit anti-glyceraldehyde 3-phosphate dehydrogenase (GAPDH) antibody (Abcam #ab181602, 1:6000); mouse anti-GSH antibody (Millipore #MAB5310, 1:1000) and rabbit anti-pyruvate dehydrogenase kinase 2 (PDK2) antibody (Abcam #ab68164, 0.5 μg/ml). Primary antibodies were diluted in Odyssey blocking buffer containing 0.01% Tween 20. Secondary antibodies [Alexa Fluor 680 goat anti-mouse IgG H&L (Life Technologies) and IRdye 800 CW goat anti-rabbit IgG H&L (LI-COR Biosciences)] were diluted in Odyssey blocking buffer (1:10 000) containing 0.02% sodium dodecyl sulphate (SDS).

## Cardiomyocyte preparation and treatment

Cardiomyocytes were purified as previously described [25]. Cardiomyocytes were incubated in the presence or absence of hydrogen peroxide ($H_2O_2$, 1–100 μM), *t*-butylhydroperoxide (TBH, 1 mM), menadione (25 μM) or diamide (0.5 mM) in incubation buffer [156 mM NaCl, 2 mM KCl, 2 mM $MgSO_4$, 1.25 mM $K_2HPO_4$, 2 mM $CaCl_2$, 10 mM 4-(2-hydroxyethyl)-1-piperazineethanesulfonic acid (HEPES), 10 mM D-glucose, pH 7.4] for 30 min at 37°C. The reaction was stopped by perchloric acid (PCA, 3.5% final). PCA precipitates were collected by centrifugation (21 000 ***g*** for 20 min at 4°C) and resolubilised in solubilisation buffer [100 mM Tris–HCl (pH 7.5), 5 mM ethylenediaminetetraacetic acid (EDTA), 0.5% SDS and 8 M urea] supplemented with 25 mM *N*-ethylmaleimide (NEM) before Western blot analysis.

## Generation of HEK293/pantothenate kinase 1β cell line

The pET28a-LIC containing human Pank1β (pantothenate kinase 1β) insert was purchased from Addgene. The insert lacks the first 28 bases and the last 3 bases of the full-length human Pank1β coding sequence. The missing bases were introduced by PCR using the following primers which were also designed to introduce an EcoR1 restriction site at the 5′-terminus and a Not1 restriction site at the 3′-terminus of the amplified sequence: 5′-GATCAGAATTCACCATGAAGCTTATAAATGGCAAAAAGCAAACATTCCCATGGTTTGGCATGGAC-3′ (forward) and 5′-ACTCGGCGGCCGCTACTTGTCATCAGTCATTTTGAACAGTT (reverse). The

PCR was performed using Pfu DNA polymerase (Thermo Scientific) and DNA Engine DYAD™, Peltier Thermal Cycler (MJ Research). The PCR product was digested and cloned into pET30a using standard procedures. The plasmid was sequenced and the resulting full-length human Pank1β sequence was used for the generation of a lentiviral construct. PCR was performed with the following primers to introduce Not1 and Mlu1 restriction sites at the start and end of the sequence, respectively, as well as to introduce an N-terminal EE-tag in the expressed protein: 5′-CACAAGCGGCCGCACCATGGAGTTCATGCCGATGGAGAAGCTTA TAAATGGCAAAAAGCAA-3′ (forward) and 5′-CACGGACGCGTCTACTTGTCATCAGTCATTTTGA-3′ (reverse). The amplified sequence was purified by ethanol precipitation, digested with Not1 and Mlu1 (New England Biolabs) and ligated into pLEX vector (Invitrogen) using the T4 Rapid ligation kit (Thermo Scientific). The plasmid was propagated in XL10-Gold *Escherichia coli* competent cells (Agilent Technologies), purified using the QIAprep Spin Miniprep Kit (Qiagen) and used for transfection. HEK293 cells at 70–80% confluence, on 10 cm tissue culture plates were co-transfected with 5.4 µg of pLEX/Pank1β or pLEX-MCS (empty vector), and 3.5 µg of pLP-1, 1.3 µg of pLP-2 and 1.8 µg of VSVG packaging plasmids using ExGene500 (Invitrogen). The the next day, culture medium containing ExGene500/DNA complexes was removed and replaced with 10 ml of complete culture medium without antibiotics. Cells were incubated at 37°C for 48 h and culture medium containing recombinant lentiviruses was collected, filtered through a Millex-HV 0.45 µm syringe filter and stored at −80°C. The stable cell lines were generated using puromycin selection. HEK293 cells were cultured in 6-well tissue culture plates to reach 50–60% confluence on the day of infection. 1 ml of the viral stock was added directly into the wells pre-filled with 1 ml of fresh Dulbecco's Modified Eagle's Medium (DMEM), and cells were incubated at 37°C, 5% $CO_2$. After 48 h, culture medium containing lentivirus was removed and replaced with selection medium (DMEM with 2 µg/ml puromycin). At the end of the selection procedure, stable overexpression of Pank1β protein expression was confirmed by Western blot using an anti-EE antibody.

## Treatment of HEK293/Pank1β cells

Approximately 0.4–1 million HEK293 or HEK293/Pank1β cells were seeded onto 60 mm culture dishes and allowed to grow for 24 h in DMEM (Lonza) supplemented with 10% foetal bovine serum (FBS, Hyclone), 50 U/ml penicillin and 0.25 µg/ml streptomycin (Lonza). The medium was replaced with pyruvate-free DMEM supplemented with 5 mM glucose and 10% FBS, and cells were incubated for a further 24 h. Cells were then treated with $H_2O_2$ (0.5 mM), menadione (50 µM), phenylarsine oxide (PAO, 10 µM), diamide (0.5 mM) and TBH (1 mM) for 30 min at 37°C in pyruvate-free DMEM supplemented with 5 mM glucose. For the recovery experiments, after incubation with $H_2O_2$ or diamide as above, cells were washed with and left to recover for up to 90 min in pyruvate-free DMEM supplemented with 5 mM glucose. For testing the effect of antioxidants, cells were incubated with 5 mM *N*-acetylcysteine or 1 mM Vitamin C in pyruvate-free DMEM supplemented with 5 mM glucose 2 h prior to diamide treatment (0.5 mM, 30 min). For testing the effect of nutrients, cells were incubated in pyruvate-free DMEM supplemented with glucose (0–40 mM), pyruvate, galactose, lactate or Vitamin C (all at 5 or 20 mM) for 18 h. After treatments, cells were collected by pressure washing and centrifugation (956 *g* for 5 min at 4°C). The medium was removed and cells were lysed in ice-cold lysis buffer (homogenisation buffer containing 1% Triton X-100) supplemented with protease inhibitor cocktail (PIC) and 25 mM NEM. Lysates were centrifuged at 21 000 *g* for 5 min at 4°C and the supernatant was analysed by Western blotting.

## Transient transfection and immunoprecipitation

HEK293 and HEK293/Pank1β cells were transfected with Origene's pCMV6-Entry vectors encoding FLAG-tagged full-length human GAPDH, creatine kinase (CK), isocitrate dehydrogenase 2 (IDH2) or PDK2 using the Turbofect transfection reagent (Thermo Scientific) according to the manufacturer's instructions. FLAG-tagged proteins were immunoprecipitated from cell lysates (lysis buffer + 25 mM NEM) using an anti-FLAG antibody (Sigma–Aldrich) and Protein G Sepharose. Endogenous HMG-CoA synthase 2 (HMGCS2) and 3-ketoacyl-CoA thiolase (ACAA2) were immunoprecipitated using rabbit monoclonal antibodies to HMGCS2 and ACAA2. Immunoprecipitated proteins were eluted with 2× loading buffer supplemented with 25 mM NEM and analysed by anti-CoA western blots.

## Western blotting

Samples of tissue/cell lysates containing ∼30–40 µg of proteins were mixed with SDS loading buffer [final concentrations: 63 mM Tris–HCl (pH 6.8), 10% glycerol, 2% SDS and 0.0025% bromophenol blue] with or

without dithiothreitol (DTT, 100 mM final) and heated for 5 min at 99°C. Resolubilised protein samples from cardiomyocytes were incubated in loading buffer and DTT at room temperature (RT) for 10 min. Proteins were separated by SDS-polyacrylamide gel electrophoresis (PAGE) on 4–20% Mini-PROTEAN TGX Precast Gels (Bio-Rad Laboratories) and transferred to low-fluorescence polyvinylidene fluoride (PVDF) membranes (Bio-Rad Laboratories). Membranes were blocked with Odyssey blocking buffer (LI-COR Biosciences). Protein bands were visualised using infrared dye-conjugated secondary antibodies and the Odyssey infrared imaging system (Odyssey Scanner CLx and Image Studio Lite software, LI-COR Biosciences).

## Animals

Animals used were male Sprague–Dawley rats (120–300 g) bred at University College London. All experiments involving animals were performed in accordance with the European Convention for the Protection of Vertebrate Animals used for Experimental and Other Scientific Purposes (CETS no.123) and the UK Animals (Scientific Procedures) Act 1986 amendment regulations 2012.

## Heart perfusion

Heart perfusion was performed as previously described except that 11 mM glucose and 1.8 mM $CaCl_2$ were added to Krebs–Henseleit bicarbonate (KHB) and bovine serum albumin (BSA) was omitted [26]. Hearts were perfused with KHB for 10 min followed by 20 min perfusion with KHB in the presence or absence of 100 μM $H_2O_2$. Hearts were freeze-clamped with tongs pre-cooled in liquid $N_2$. Frozen hearts were powdered in liquid $N_2$ and homogenised in ice-cold homogenisation buffer [50 mM Tris–HCl (pH 7.5), 150 mM NaCl, 5 mM EDTA, 50 mM NaF and 5 mM $Na_4P_2O_7$] supplemented with 25 mM NEM and PIC (Roche) using a tissue disintegrator. Triton X-100 was added (1% final) and the homogenate was mixed well before centrifuging at 21 000 *g* for 5 min at 4°C. The supernatant was analysed by Western blotting.

## Liver sample preparation

Rats were starved for 24 h with constant access to water or fed a high-fat/high-sucrose (HF/HS) diet containing 35.5% fat and 36.6% carbohydrate for a week (D09071702, Research Diets, Inc.). Rats were anaesthetised with pentobarbitone (300 mg/kg of body weight), and livers were removed and immediately freeze-clamped using tongs pre-cooled in liquid $N_2$. Frozen livers were powdered in liquid $N_2$ and homogenised in ice-cold homogenisation buffer supplemented with 25 mM NEM and PIC using a tissue disintegrator. SDS was added (1% final), and the homogenate was sonicated to reduce viscosity before centrifuging at 21 000 *g* for 5 min at RT. The supernatant was analysed by western blotting.

## Enzyme activity assays

CK (rabbit muscle, Roche #127 566; 7.2 μg/ml) was incubated with or without 10 mM CoASSCoA (CoA disulphide) or GSSG in 50 mM Tris–HCl (pH 7.5) at RT for 20 min. Samples were then incubated with or without DTT (45 mM final) at RT for 5 min. A 5 μl aliquot of the incubation mixture was diluted to a final volume of 200 μl with assay buffer which consisted of hexokinase 3.3 mU/ml (yeast, Roche #1 426 362), 1.7 μg/ml GAPDH (yeast, Roche catalogue #127 655), 2 mM NADP, 2 mM ADP, 20 mM glucose, 2 mM EDTA, 10 mM magnesium acetate, 422.5 mM triethanolamine (TEA; pH 7.6) and 60 mM phosphocreatine. CK activity was determined by measuring the increase in absorbance of NADPH at 340 nm at 30°C for 10 min using a Tecan plate reader.

GAPDH (rabbit muscle, Sigma–Aldrich #G2267) was incubated at 15 μg/ml with or without 10 mM CoASSCoA or GSSG in the presence or absence of 15 mM DTT in 70 mM $KH_2PO_4$ (pH 7.6) for 1 min on ice. A 5 μl aliquot of the incubation mixture was diluted to a final volume of 150 μl with assay buffer which consisted of 82.6 mM $KH_2PO_4$ (pH 7.6), 6.6 mM 3-phosphoglyceric acid, 1.1 mM ATP, 20 μM NADH, 0.9 mM EDTA, 1.6 mM $MgSO_4$ and 29.2 μg/ml 3-phosphoglyceric phosphokinase (from Baker's yeast, Sigma–Aldrich #P7634). The assay buffer was incubated at 30°C for 10 min before the addition of GAPDH. GAPDH activity was determined by measuring the decrease in absorbance of NADH at 340 nm at RT for 10 min using a Tecan plate reader.

NADP-dependent IDH from porcine heart (Sigma–Aldrich #I1877) (1.1 mg/ml) was incubated with or without 10 mM CoASSCoA or GSSG in the presence or absence of 20 mM DTT in 30 mM Tris–HCl (pH 7.5), 90 mM NaCl, 0.6 mM $MgCl_2$ and 0.6 mM $MnCl_2$ at RT for 20 min. A 5 μl aliquot of the incubation mixture was assayed in 190 μl of assay buffer consisting of 34 mM Tris–HCl (pH 7.5), 102 mM NaCl, 1.37 mM $MgCl_2$,

0.13 mM NADP$^+$ and 0.13 mM isocitrate. The reaction was started by the addition of isocitrate, and NADP-dependent IDH activity was determined by measuring the increase in absorbance of NADPH at 340 nm at RT for 10 min using a Tecan plate reader.

## PDK2 assay

HEK293 cells were transfected with pCMV6-Entry/FLAG-PDK2; 48 h after transfection, cells were collected and lysed in reducing lysis buffer [50 mM Tris–HCl (pH 7.5), 150 mM NaCl, 5 mM EDTA, 50 mM NaF, 5 mM Na$_4$P$_2$O$_7$, 1% Triton X-100, PIC and 1 mM DTT]. The lysate was centrifuged at 21 000 *g* for 10 min at 4°C, and the concentration of the supernatant was measured by the Bradford assay. The protein and DTT concentrations of the supernatant were adjusted with lysis buffer to 3 mg/ml and 0.5 mM, respectively, and 0.15 ml was incubated with 2 µg of anti-FLAG antibody (Sigma–Aldrich) and 10 µl of Protein G Sepharose for 4 h at 4°C. The immunoprecipitates were collected by centrifugation (956 *g* for 30 s) and washed/recentrifuged once with 0.4 ml of lysis buffer without DTT and then with 0.2 ml of TBS. The immunoprecipitates were incubated with or without 1 mM GSSG or CoASSCoA in 50 µl of TBS for 20 min at RT. Beads were pelleted by centrifugation (956 *g* for 30 s) and washed/recentrifuged twice with 0.4 ml of cold TBS. FLAG-PDK2 was eluted by incubating the beads for 30 min at 4°C with 15 µl of PDK2 elution buffer [50 mM KH$_2$PO$_4$ (pH 7.6), 0.3 mM EDTA, 10 mM 2-glycerophosphate and 0.2 mg/ml FLAG peptide (Sigma–Aldrich)]. Beads were pelleted by centrifugation as above and 15 µl of the supernatant was collected and mixed with 10 µl of pyruvate dehydrogenase (PDH; from porcine heart, Sigma–Aldrich #P7032) that had been diluted to 1.3 mg/ml in 10 mM Tris–HCl (pH 7.5) and desalted twice using desalting spin columns (MWCO 7000 Da, Thermo Scientific). PDK2 activity was measured by the incorporation of $^{33}$P from γ-$^{33}$P ATP (New England Nuclear) into the E1 subunit of the PDH complex in the presence or absence of 2 mM DTT. The reaction was started by the addition of 5 µl of ATP/Mg mix (150 µM ATP, 2 µCi γ-$^{33}$P ATP and 30 mM MgCl$_2$). After incubating for 10 min at RT, the reaction was stopped by the addition of 14 µl of 4× loading buffer and 2 µl of 300 mM DTT. Samples were heated at 99°C for 5 min and proteins were separated by SDS–PAGE. The incorporation of $^{33}$P into PDH was visualised by autoradiography (Fuji Film Image Reader FLA-2000), and band intensities were quantified using the MultiGauge software.

## Quantification of CoA in cells and tissues

These were measured by HPLC as previously described, except that 3.5% PCA was used to extract CoA from tissues/cells and EDTA was omitted from the injection mixture [27].

## Quantification of protein-bound CoA

HEK293/Pank1β cells were treated with various oxidising agents and collected as described. Cells were lysed in 0.3 ml of lysis buffer supplemented with PIC, 25 mM NEM and 1% SDS, and sonicated to reduce viscosity. Lysates were centrifuged at 21 000 *g* for 5 min at RT and proteins in the supernatant were precipitated by the addition of methanol (80% final, v/v). Samples were vigorously vortexed and centrifuged at 21 000 *g* for 3 min. The supernatant was discarded and the pellet was washed with 1 ml of 80% methanol using a handheld tissue tearor (Biospec Products). Proteins were pelleted again by centrifugation (21 000 *g* for 5 min at room temperature), the supernatant was discarded and the pellet was washed again as above. Proteins were pelleted again by centrifugation (21 000 *g* for 5 min at room temperature) and the supernatant was discarded. Residue methanol was removed by placing samples in a heating block for a few minutes. The pellet was solubilised in 45 µl of reducing resolubilisation buffer consisting of 89 mM TEA, 0.44 mM KOH and 11.1 mM DTT by gentle sonication. After incubation for 5 min at RT, proteins were precipitated by the addition of 22 µl of 5% PCA and pelleted by centrifugation at 21 000 *g* for 10 min at 4°C. The supernatant was collected, and the pH was adjusted to 6–7 with 0.5 M K$_2$CO$_3$ and centrifuged again at 21 000 *g* for 10 min at 4°C. A 50 µl aliquot of the supernatant was used for CoA measurement by a modification of the recycling assay described by Allred and Guy [28] as follows. Neutralised samples were made up to a total volume of 160 µl in wells of a 96-microtiter plate which additionally contained 375 mM Tris–HCl (pH 7.2), 75 mM KCl, 15 mM malate, 6 mM acetylphosphate, 1.5 mM NAD$^+$, malate dehydrogenase (1 unit) and citrate synthase (1 unit). After incubation at RT for 10 min, the reaction was started by the addition of 40 µl of phosphotransacetylase (3.5 units) and the rate of NADH production at 30°C was monitored for 20 min at 340 nm using a Tecan plate reader. The amounts of CoASH in samples were determined by measuring the rate of NADH production by CoA standard (Sigma–Aldrich) diluted in reducing buffer which had been treated with 5% PCA and neutralised as described above. To

determine the total amount of protein from which CoA was released, the PCA pellets were washed with 1 ml of 0.1% PCA and resuspended in 0.2 ml of resolubilisation buffer by sonication, and protein concentration was determined by the BCA assay (Thermo Scientific).

## CoASSG preparation

CoASSG was produced by incubating oxidised GSH with reduced CoA in 50 mM Tris–HCl (pH 8) for 30 min at 30°C. The reaction mixture was analysed by HPLC under the same conditions as those used for CoA measurements [27]. The GSSCoA peak was collected and desalted with a PD10 column (MWCO700, GE Healthcare).

## Purification and activity assay of Nudix 7 hydrolase

Recombinant His-Nudix 7 hydrolase was expressed in bacteria and purified by Ni-NTA affinity chromatography. His-Nudix 7 (1.7 $\mu$g) was incubated in a total volume of 100 $\mu$l containing 50 mM $(NH_4)HCO_3$ and 0.2 mM CoASSG at 37°C for 20 min with or without 5 mM $MgCl_2$. Reaction products and substrates were analysed by HPLC as described except that elution was monitored at 205 nm [27]. Peaks for 3′,5′-ADP, 4-phosphopantetheinyl GSH and CoASSG were identified by comparison of retention times with those of authentic standards.

## Preparation and enrichment of CoAlated peptides from $H_2O_2$-treated heart for MS analysis

Frozen, powdered heart was homogenised in ice-cold buffer containing 10 mM 3-[4-(2-hydroxyethyl)-1-piperazinyl] propanesulfonic acid, 150 mM NaCl, 1 mM EDTA, 1 mM NaF, 1 mM $Na_3VO_4$, 10 mM $Na_4P_2O_7$, 1 mM 2-glycerophosphate, 25 mM NEM and PIC using a tissue disintegrator. Triton X-100 was added (1% final), and the homogenate was mixed well and centrifuged at 21 000 $g$ for 3 min at 4°C. Proteins in the supernatant were precipitated with 90% methanol. The protein pellet was resuspended in 50 mM $(NH_4)HCO_3$ (pH 7.8) supplemented with 6.4 mM iodoacetamide (IAM) and digested with Lys C and trypsin (sequencing grade, Promega). The digestive enzymes were heat-inactivated (99°C, 10 min) and CoAlated peptides were immunoprecipitated with anti-CoA antibody cross-linked to Protein G Sepharose. Immunoprecipitated peptides were eluted with 0.1% trifluoroacetic acid and dried completely in a speed vac concentrator. The resulting pellet was resolubilised in 50 mM $(NH_4)HCO_3$ and 5 mM $MgCl_2$, and 1.7 $\mu$g of Nudix 7 was added. The solution was incubated at 37°C for 20 min and then acidified, desalted with a C18 Stage tip that contained 1.5 $\mu$l of Poros R3 resin and partially dried in a speed vac concentrator before LC–MS/MS analysis.

## Preparation and enrichment of CoAlated peptides from liver mitochondria for MS analysis

Liver mitochondria were prepared using a modification of the method by Fernández-Vizarra et al. [29]. Briefly, pieces of liver were homogenised in isolation buffer (0.32 M sucrose, 1 mM EDTA, 25 mM NEM and 10 mM Tris–HCl, pH 7.4) and centrifuged for 5 min at 1000 $g$ at 4°C. The supernatant was collected and centrifuged for 2 min at 15 000 $g$ at 4°C. The pellet was resuspended in isolation buffer and centrifuged again as above, and the resulting pellet containing mitochondria was snap-frozen and stored in liquid $N_2$. Mitochondria were lysed in lysis buffer supplemented with 25 mM NEM and PIC and centrifuged at 21 000 $g$ for 10 min at 4°C. Soluble proteins were separated by SDS–PAGE as above, and the 37–50 kDa area was cut out and proteins were eluted in elution buffer [50 mM Tris–HCl (pH 7.5), 150 mM NaCl, 0.1 mM EDTA, 0.1% SDS and 20 mM NEM] on a rotating wheel for 6 h at 4°C. Eluted proteins were precipitated and washed with 90% methanol. The protein pellet was digested with trypsin and CoAlated peptides were immunoprecipitated using anti-CoA antibody as above. Immunoprecipitated peptides were treated with Nudix 7 and enriched further by an IMAC column before LC–MS/MS analysis.

## Mass spectrometry data acquisition

The enzymatic digests were analysed by nano-scale capillary LC-MS/MS using an Ultimate U3000 HPLC (ThermoScientific Dionex, San Jose, USA) to deliver a flow of approximately 300 nl/min. A C18 Acclaim PepMap100 5 $\mu$m, 100 $\mu$m × 20 mm nanoViper (ThermoScientific Dionex, San Jose, USA) trapped the
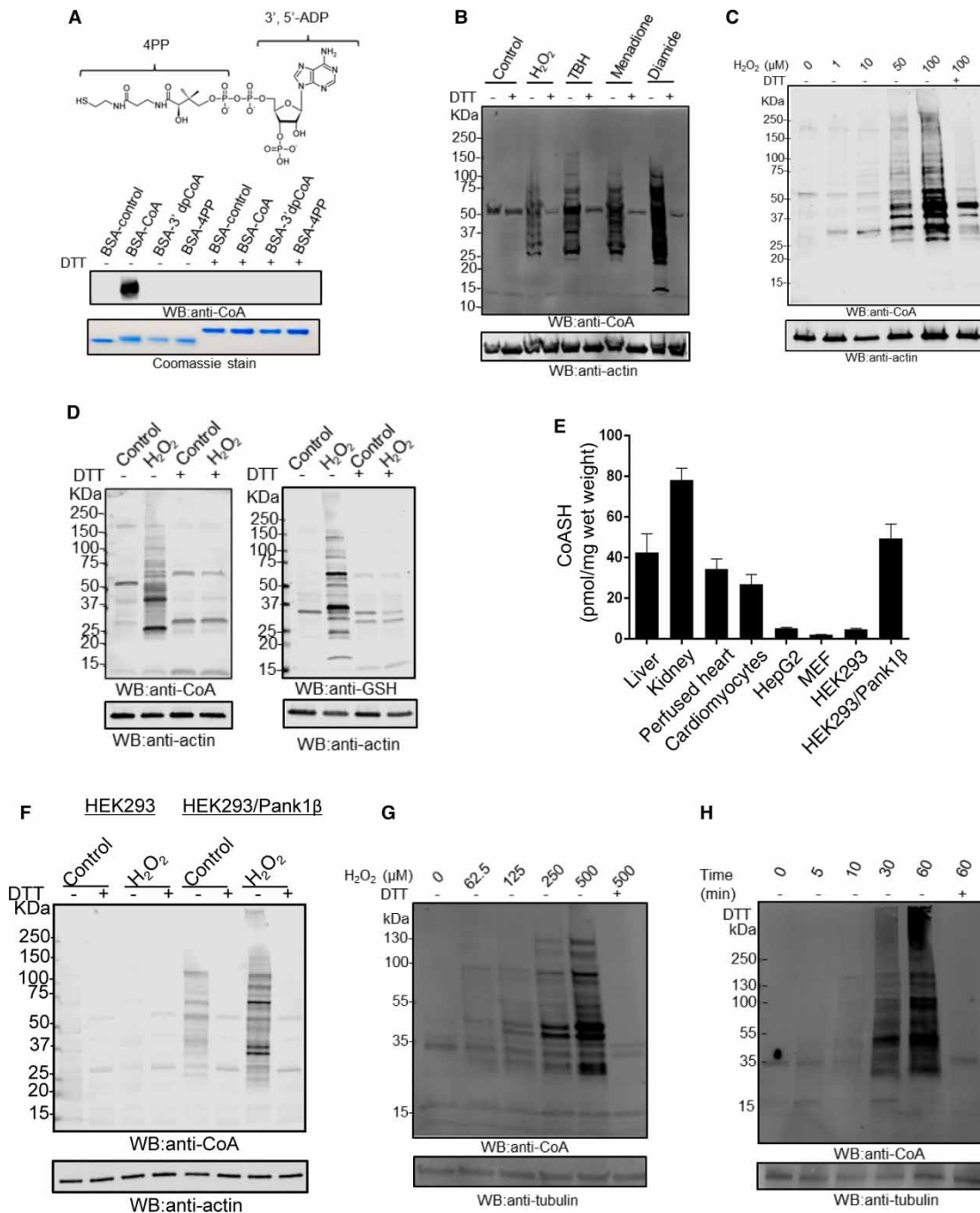
**Figure 1. Protein CoAlation is induced by oxidative stress in mammalian cells and the extent of modification is determined by cellular levels of CoA.**
                                                                                                    Part 1 of 2

(**A**) Top, structure of CoA. Bottom, western blot demonstrating specificity of anti-CoA antibody. CoA, dpCoA and 4PP were conjugated to BSA through disulphide linkage and analysed by anti-CoA immunoblot in the presence and absence of DTT. (**B**) Anti-CoA western blot reveals extensive modification of cellular proteins by CoA in rat cardiomyocytes in response to various oxidising agents. (**C**) Adult rat cardiomyocytes were untreated or treated with the indicated concentrations of $H_2O_2$ for 30 min, and protein CoAlation was examined by anti-CoA immunoblot. (**D**) The patterns of proteins modified by CoAlation and glutathionylation in response to $H_2O_2$ are distinct. Isolated rat hearts were perfused in the presence or absence of 100 $\mu$M $H_2O_2$ for 20 min, and protein CoAlation and glutathionylation were examined by immunoblotting with anti-CoA or anti-GSH monoclonal antibodies. (**E**) Comparison of CoA levels in rat tissues, primary and established cell lines. Data are mean ± SEM of

peptides prior to separation on a C18 Acclaim PepMap100 3 μm, 75 μm × 250 mm nanoViper (ThermoScientific Dionex, San Jose, USA). Peptides were eluted with a gradient of acetonitrile. The analytical column outlet was directly interfaced via a modified nano-flow electrospray ionisation source, with a hybrid dual pressure linear ion trap mass spectrometer (Orbitrap Velos, ThermoScientific, San Jose, USA). Data dependent analysis was carried out, using a resolution of 60,000 for the full MS spectrum, followed by 20 MS/MS spectra in the linear ion trap. MS spectra were collected with an automatic target gain control of $1 \times 10^6$ and a maximum injection fill time of 250 ms over a $m/z$ range of 350–1600. MS/MS scans were collected using an automatic gain control value of $1 \times 10^4$ and a threshold energy of 35 for collision induced dissociation. The Orbitrap measurements were internally calibrated using the lock mass of polydimethylcyclosiloxane at $m/z$ 445.120025.

## Data processing

LC–MS/MS raw data files were processed as a single unlabelled sample using MaxQuant [30] version 1.5.2.8, which incorporates the Andromeda search engine. For all data sets, the default parameters in MaxQuant were used, except for MS/MS tolerance at 0.6 Da and that the second peptide ID was unselected. Carbamidomethylation of cysteine and the N-terminus, N-ethylmaleimide cysteine, oxidation of methionines, CoAlation of cysteine with delta mass values 338, 356 and 765 were allowed as variable modifications. MaxQuant-processed data were searched against a protein sequence database (Uniprot KB-human, June 2013) database.

Using MQ viewer, CoA_356 peptides were first visually checked and those MS/MS scans that 'failed' visually were checked manually. The corresponding MS/MS scan was manually sequenced to match the identified peptide.

## Statistical analysis

Where appropriate, values are given as means ± SEM. Statistical significance was determined by a one-way or two-way ANOVA with correction for multiple comparisons as specified in the figure legends. Differences were considered significant at the 5% level. Graphs were produced and statistics were calculated using GraphPad Prism version 6.07 for Windows (GraphPad Software, La Jolla, CA, U.S.A., www.graphpad.com).

# Results

## Extensive modification of cellular proteins by CoA in response to oxidative stress

The identification of the post-translational modification of cellular proteins by CoA has been hampered by the lack of specific antibodies that would allow its detection, in contrast with the availability of protocols to study phosphorylated, acetylated or glutathionylated proteins. We have recently developed a highly specific anti-CoA monoclonal antibody 1F10 which recognises CoA in various immunological assays [24]. Western blot analysis of BSA alone and the BSA-CoA, BSA-dpCoA and BSA-4PP (4′-phosphopantetheine) disulphide conjugates with 1F10 antibody showed specific recognition of BSA-CoA in a DTT-sensitive manner (Figure 1A). Since the BSA-dpCoA disulphide conjugate is not recognised by the 1F10 antibody, we can conclude that the 3′-phosphate of the deoxyribose ring is part of the epitope for the given antibody. Further characterisation of this antibody in western blot analysis of protein extracts from mammalian cells and tissues revealed under non-reducing conditions many immunoreactive bands, suggesting covalent binding of CoA to cellular proteins. The above findings and the identification of several eukaryotic and prokaryotic proteins with covalently bound CoA [23,20,21] prompted us to investigate in mammalian cells and tissues the extent of protein thiol

**Figure 1. Protein CoAlation is induced by oxidative stress in mammalian cells and the extent of modification is determined by cellular levels of CoA.**

Part 2 of 2

at least three biological replicates ($n = 5$ for cardiomyoctes and HEK293; $n = 4$ for HepG2 (hepatocellular carcinoma) and MEF (mouse embryonic fibroblasts); $n = 3$ for the rest). (**F**) Protein CoAlation is induced by $H_2O_2$ in HEK293/Pank1β, but not in parental HEK293 cells. (**G**) HEK293/Pank1β cells were incubated with the indicated concentrations of $H_2O_2$ for 10 min, and protein CoAlation was examined by anti-CoA immunoblot. (**H**) HEK293/Pank1β cells were incubated with 250 μM $H_2O_2$ for the indicated times, and protein CoAlation was examined by anti-CoA immunoblot.

modification by CoA (which we have termed CoAlation) under various experimental conditions. Initially, we examined whether oxidising agents can induce protein CoAlation in primary adult rat cardiomyocytes, which contain high levels of CoA. The treatment of isolated cardiomyocytes for 30 min with the oxidising agents $H_2O_2$, TBH or menadione, or with the thiol-selective oxidant diamide, all resulted in extensive immunoreactivity with the anti-CoA antibody when cell lysates were examined by western blot under non-reducing conditions (Figure 1B). Notably, most of the immunoreactive bands were not detected when protein samples were separated under reducing conditions (100 mM DTT), suggesting the formation of mixed disulphides between CoA and cellular proteins. There was one major DTT-insensitive immunoreactive band, which is likely to be due to non-specific binding of antibodies. To further validate these findings, isolated cardiomyocytes were treated with increasing concentrations of $H_2O_2$. As shown in Figure 1C, treatment of cardiomyocytes with $H_2O_2$ increased protein CoAlation in a dose-dependent manner, with the effect being most pronounced at 100 $\mu$M $H_2O_2$, while several immunoreactive bands were detected at as low as 1 $\mu$M $H_2O_2$.

These findings encouraged us to employ the Langendorff-perfused heart model for studying protein CoAlation in rat heart exposed to oxidative stress. This model has been employed extensively to study redox regulation and protein S-thiolation. We found that perfusing rat hearts with 100 $\mu$M $H_2O_2$ for 20 min significantly increased protein CoAlation, which was reversed to the level of untreated control by DTT (Figure 1D). Immunoblotting the same samples with anti-GSH monoclonal antibody D8 also showed extensive glutathionylation of cellular proteins in a DTT-sensitive manner (Figure 1D). Interestingly, the patterns of proteins modified by these post-translational modifications varied significantly, suggesting differential targeting of cysteine thiols in cellular proteins by CoA and GSH in response to oxidative stress.

Analysis of CoASH concentrations in rat tissues, and primary and established cell lines revealed that primary cardiomyocytes, kidney, liver and heart contain much higher concentrations of CoASH when compared with HepG2 and HEK293 (Figure 1E). We were interested to find whether the extent of protein CoAlation is determined by the cellular level of CoASH. The treatment of exponentially growing HEK293 cells with 500 $\mu$M $H_2O_2$ showed no significant increase in protein CoAlation (Figure 1F). To test whether increasing the concentration of CoA in HEK293 cells can augment protein CoAlation in response to $H_2O_2$, we generated HEK293 cells with stable overexpression of Pank1$\beta$. It has been shown that the overexpression of Pank1$\beta$, the main rate-limiting enzyme in CoA biosynthesis, significantly increases CoA levels in Cos7 cells [31]. A markedly increased protein CoAlation was observed in HEK293/Pank1$\beta$ cells treated with 500 $\mu$M $H_2O_2$ (Figure 1F). Many proteins were also CoAlated in untreated cells. As in cardiomyocytes, the effect of $H_2O_2$ on protein CoAlation in HEK293/Pank1$\beta$ cells was dose-dependent (Figure 1G). In a time-course study, we found that CoAlated proteins are detected in HEK293/Pank1$\beta$ cells as early as 5 min after $H_2O_2$ treatment (Figure 1H).

The HEK293/Pank1$\beta$ cell model was further used to examine protein CoAlation in response to a diverse range of oxidising agents. The present study revealed extensive protein CoAlation in response to $H_2O_2$, diamide, menadione and TBH; however, only a few proteins were shown to be CoAlated in cells treated with PAO to block vicinal dithiols (Figure 2A). The extensive protein CoAlation in response to several oxidising agents led us to quantify the level of protein-bound CoA in HEK293/Pank1$\beta$ cells treated with or without oxidising agents. The determined values of protein-bound CoA (Figure 2B) correlated to the intensity of anti-CoA immunoreactive bands in HEK293/Pank1$\beta$ cells treated with the same panel of oxidising agents (Figure 2A). A low level of CoA ($30 \pm 3$ pmol/mg$_{protein}$, $n = 6$) was extracted from the total protein of untreated cells, while treatment with oxidising agents resulted in a 2- to 12-fold increase in protein-bound CoA ($H_2O_2$: $98 \pm 2$ pmol/mg$_{protein}$ $n = 3$; menadione: $149 \pm 7$ pmol/mg$_{protein}$ $n = 3$; PAO: $58 \pm 4$ pmol/mg$_{protein}$ $n = 6$; diamide: $355 \pm 14$ pmol/mg$_{protein}$, $n = 6$; TBH: $135 \pm 11$ pmol/mg$_{protein}$ $n = 3$).

## Protein CoAlation is a reversible post-translational modification

Covalent protein modifications, such as phosphorylation, acetylation and glutathionylation, are reversible regulatory events. To establish whether protein CoAlation is a reversible post-translational modification, HEK293/Pank1$\beta$ cells were treated with 500 $\mu$M $H_2O_2$ for 60 min and then left to recover for various periods of time in complete growth medium. As shown in Figure 2C, the $H_2O_2$-mediated increase in protein CoAlation in HEK293/Pank1$\beta$ cells was reversed to basal levels in a time-dependent manner. Surprisingly, a significant decrease in protein CoAlation occurs within 5 min after removal of $H_2O_2$ and reaches baseline levels within 90 min. The reversibility of protein CoAlation was also observed in diamide-treated HEK293/Pank1$\beta$ cells after the removal of the oxidising agent (Figure 2D). These data suggest that protein de-CoAlation is a fast event initiated as soon as the oxidative stress is removed.
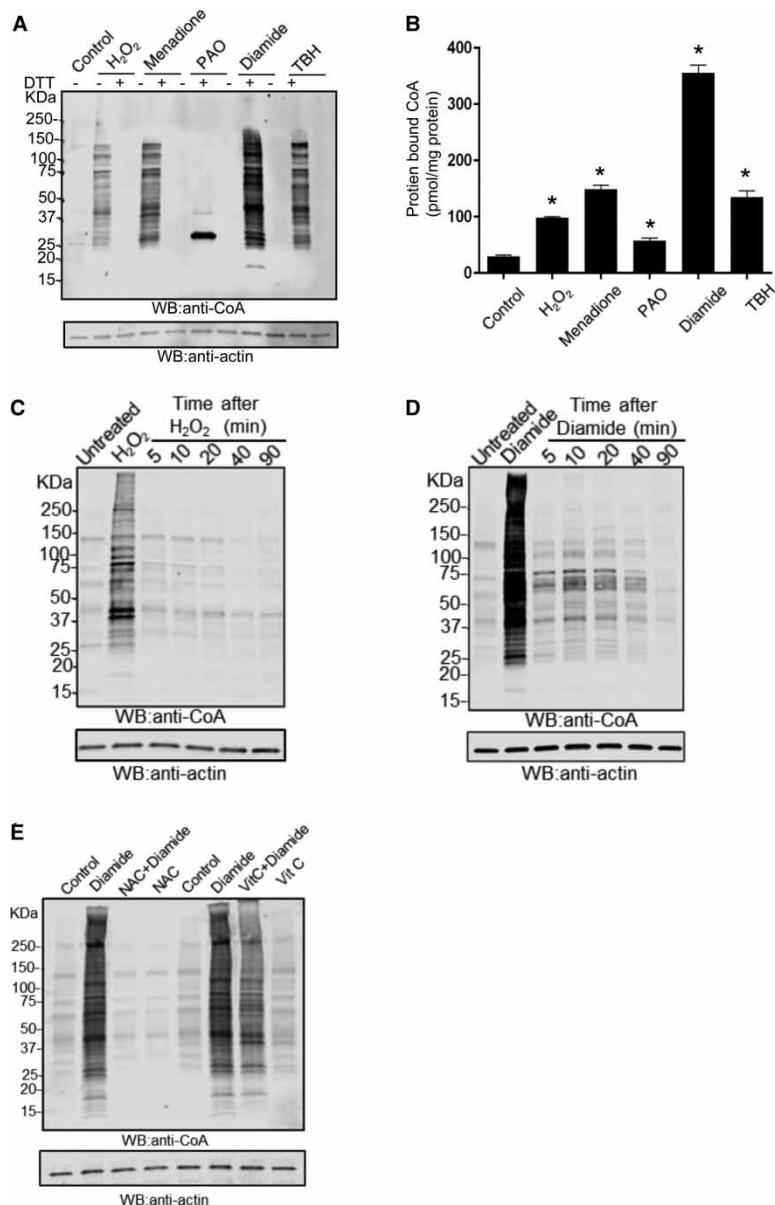
**Figure 2. Protein CoAlation is a reversible post-translational modification and it is prevented by antioxidants.**
(**A**) Anti-CoA western blot showing extensive protein CoAlation in HEK293/Pank1β in response to various oxidising agents.
(**B**) Quantitation of protein-bound CoA after the treatment of HEK293/Pank1β cells with oxidising agents (related to Figure 2A).
Values and error bars represent mean ± SEM of at least three independent experiments ($n = 6$ for control, PAO and diamide; $n = 3$ for the rest). *$P < 0.001$ compared with the control group by one-way ANOVA followed by Dunnett's *post hoc* analysis to correct for multiple comparisons. (**C** and **D**) Diamide- and $H_2O_2$-induced protein CoAlation in HEK293/Pank1β cells is reversed upon removal of the oxidants. HEK293/Pank1β cells were treated with 250 μM $H_2O_2$ and 0.5 mM diamide for 30 min. The medium was then replaced with fresh media without the oxidants and cells were incubated for the indicated times. Protein CoAlation was examined by anti-CoA immunoblot. (**E**) Protein CoAlation is prevented by antioxidants. HEK293/Pank1β cells were pretreated for 2 h with NAC or Vitamin C before treatment with 0.5 mM diamide for 30 min. Protein CoAlation was examined by anti-CoA western blotting.

Oxidative stress in cells is closely associated with the activation of antioxidant defence systems, which keep oxidants at an optimum level. Therefore, we examined whether protein CoAlation induced by oxidising agents could be prevented by pretreatment of cells with known antioxidants, such as *N*-acetyl-L-cysteine (NAC) and
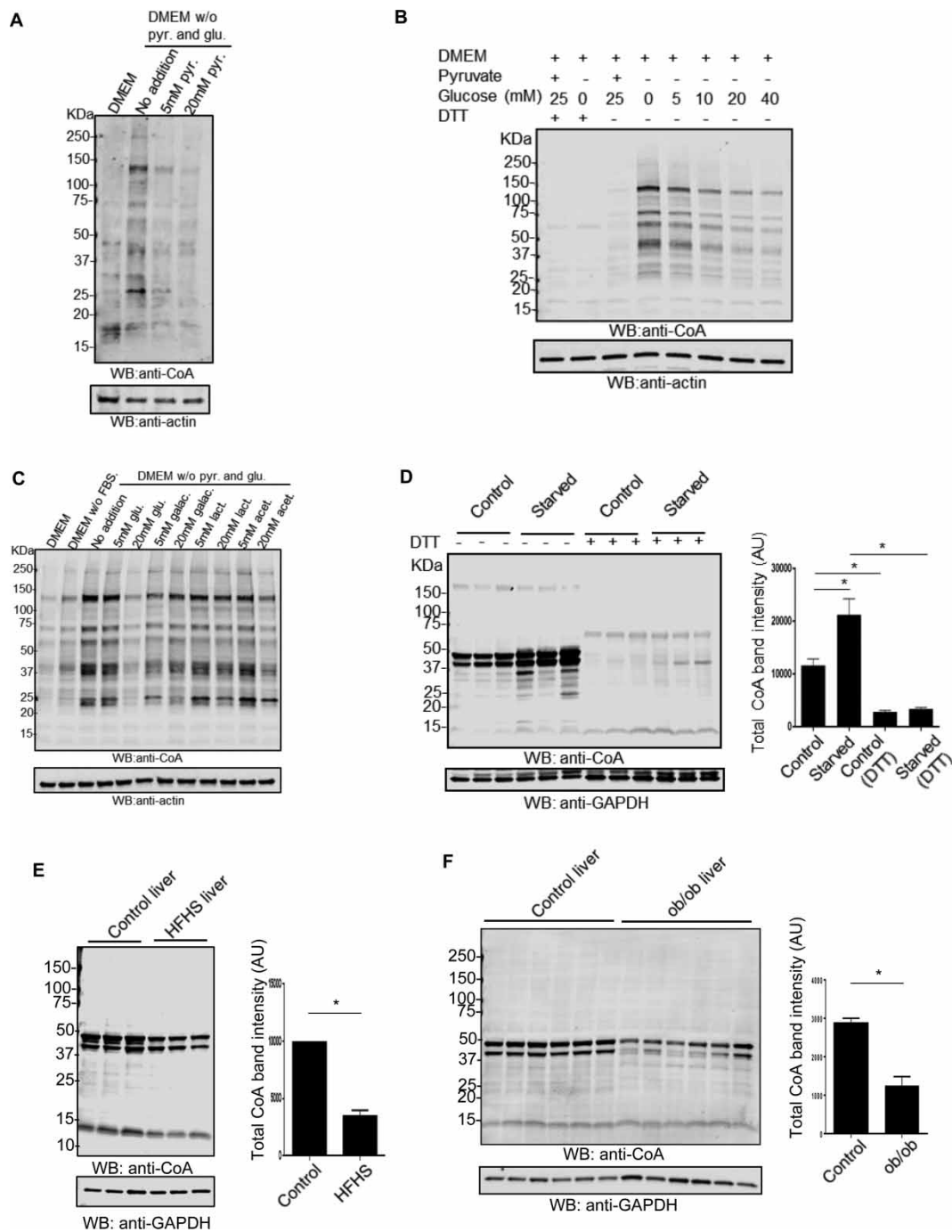
**Figure 3. Induction of protein CoAlation by metabolic stress.**
(**A**) HEK293/Pank1β cells were incubated in pyruvate (pyr) and glucose (glu)-free DMEM medium alone or supplemented with 5 or 20 mM pyruvate. Protein CoAlation was analysed by anti-CoA immunoblot. (**B**) HEK293/Pank1β cells were incubated in complete pyruvate and glucose-free DMEM alone or supplemented with different concentrations of glucose. Protein CoAlation was analysed by anti-CoA immunoblot. (**C**) HEK293/Pank1β cells were incubated in pyruvate and glucose-free DMEM alone or supplemented with different concentrations of glucose (glu), galactose (galac), lactate (lac) or acetate (acet). Protein CoAlation was analysed by anti-CoA immunoblot. (**D**) Induction of protein CoAlation in rat liver after fasting for 24 h. (**E**) Feeding HF/HS diet for 1 week reduces protein CoAlation in rat liver. (**F**) Protein CoAlation is decreased in the livers of ob/ob mice. Data are mean ± SEM of three (**D** and **E**) or six (**F**) biological replicates. *$P < 0.05$ by one-way ANOVA.

Vitamin C. We found that incubation of HEK293/Pank1β cells with 5 mM NAC for 2 h before diamide treatment largely prevented protein CoAlation induced by 0.5 mM diamide (Figure 2E). The effect of Vitamin C (1 mM) was less pronounced, resulting in ∼50% decrease in anti-CoA immunoreactivity.

## Protein CoAlation is induced by metabolic stress

We consistently observed a low level of DTT-sensitive immunoreactivity with the anti-CoA antibody when samples of exponentially growing HEK293/Pank1β cells were analysed by Western blot (Figure 1F–H). In addition, a small amount of CoA could be extracted with DTT from the total protein fraction of untreated HEK293/Pank1β cells (Figure 2B). These observations show that some proteins are CoAlated in cells even in the absence of exogenously added oxidants. Interestingly, this basal CoAlation of cellular proteins was increased in cells cultured in media lacking glucose and pyruvate (Figure 3A). The induction of protein CoAlation in pyruvate- and glucose-deprived cells was reversed by the re-addition of glucose or pyruvate, and the effect was concentration-dependent (Figure 3A,B). Moreover, galactose, lactate and acetate, which are used less efficiently by mammalian cells as an energy source, were less capable of reducing protein CoAlation in pyruvate- and glucose-deprived cells (Figure 3C). These observations led us to examine the effect of fuel utilisation and metabolic stress on protein CoAlation in animal models under physiological and pathological metabolic conditions. As shown in Figure 3D, protein CoAlation in the rat liver was significantly induced after fasting for 24 h. These results suggest that protein CoAlation is induced not only by oxidising agents, but also occurs when liver is under metabolic stress induced by starvation. Changes in protein CoAlation were also detected in the liver under pathologically relevant conditions of metabolic syndrome. We found that feeding HF/HS diet for 1 week resulted in a substantial decrease in protein CoAlation in rat liver (Figure 3E). In agreement with the above finding, protein CoAlation was also markedly decreased in the liver of genetically obese ob/ob mice compared with wild-type littermate mice (Figure 3F).

## Identification of CoAlated proteins by mass spectrometry

Extensive protein CoAlation induced by oxidising agents and metabolic stress in mammalian cells and tissues, and the availability of 1F10 antibody led us to develop a strategy for the identification of CoA-modified proteins. We have previously demonstrated that the 1F10 antibody specifically precipitated BSA-CoA conjugate, but with low efficiency [24]. Taking this into account, we prepared a CoA-glutahione disulphide (CoASSG) heterodimer and showed that the 1F10 antibody could effectively immunoprecipitate the CoASSG heterodimer in a concentration-dependent manner (results not shown). Initially, we employed the following methodology for the identification of CoAlated peptides by LC–MS/MS. Isolated rat hearts were perfused with 100 μM $H_2O_2$ for 20 min and total lysates were prepared in the presence of 25 mM NEM to block free thiols. Protein was extracted by methanol precipitation and digested with Lys-C/trypsin in the presence of IAM. Then, CoAlated peptides were immunoprecipitated with 1F10 antibody cross-linked to Protein G Sepharose. The eluted peptides were analysed by LC–MS/MS. Protein database searches using the MaxQuant Andromeda software [30], set to include a post-translational cysteine modification showing an increase in 765 Da, corresponding to covalently bound CoA (CoA: 767.535 Da), initially only returned a few matching fragment ion spectra. This was because of the fragmentation of CoAlated peptides (Cys + 765) during LC–MS/MS, giving rise to a characteristic neutral loss of $m/z$ 428 and $m/z$ 508 from the parent ion with very little peptide backbone fragmentation (Figure 4A). Therefore, to improve the identification of CoAlated peptides, we cleaved off the 3′,5′-ADP moiety of CoA responsible for the neutral loss fragment ions. To do this, CoAlated peptides were eluted from immune complexes and digested with Nudix7 (Nudix hydrolase 7). Nudix7 belongs to the family of phosphohydrolases and functions as a CoA/acyl CoA diphosphatase [32]. The LC–MS/MS analysis of CoAlated peptides digested with Nudix7 is expected to show an increase in 356 Da, corresponding to covalently attached 4PP (Figure 4B). Indeed, the digestion of immunoprecipitated CoA-modified peptides with Nudix7 results in a distinctive MS/MS fragmentation signature of Cys + 356. Representative MS/MS spectra of cysteine-containing peptides from $H_2O_2$-treated hearts are shown in Figure 4C,D.

The developed protocol allowed us to identify in rat heart perfused with 100 μM $H_2O_2$ for 20 min a total of 80 CoAlated peptides that matched to 58 proteins (Supplementary Table S1). In addition, 43 CoAlated peptides corresponding to 33 proteins were identified in the liver mitochondria prepared from a 24 h starved rat (Supplementary Table S2). Bioinformatic pathway analysis of identified proteins showed that they are implicated in a diverse range of cellular processes, including intermediate metabolism,
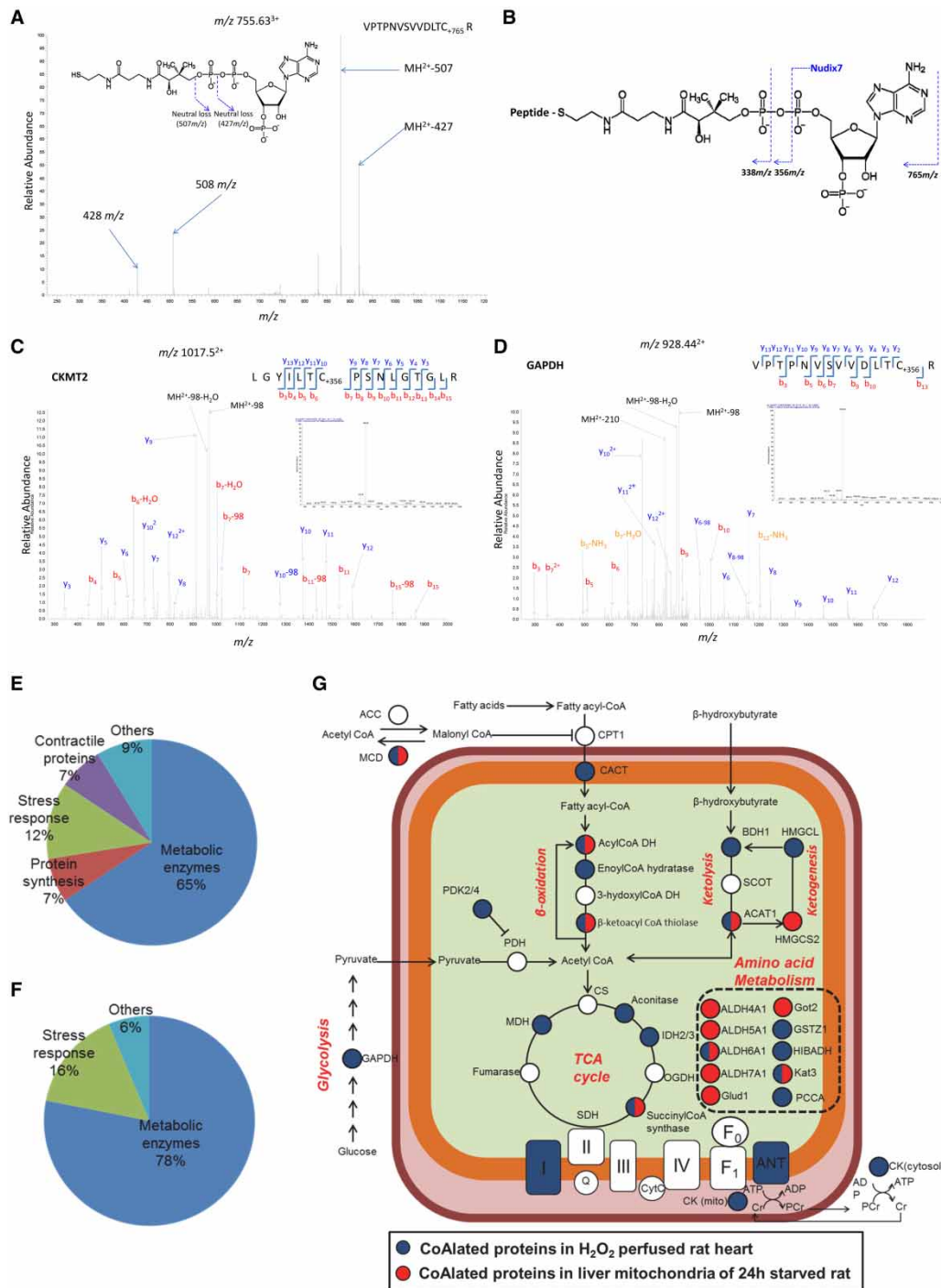
**Figure 4. Proteomic identification of CoAlated proteins in H₂O₂-treated heart and in the liver of starved rats.** Part 1 of 2
(**A**) LC–MS/MS spectrum of a CoAlated peptide derived from heart protein, showing an increase in 765 Da, corresponding to covalently bound CoA. The inset (a) shows the structure of CoA and indicates the neutral loss of the ATP moiety (*m/z* 507 and 427), which can occur under CID (collision-induced dissociation) fragmentation of the precursor ion. The major ions identifying these neutral losses are annotated on the spectrum. (**B**) Nudix7 cleaves the diphosphate bond of CoA, generating a unique signature for MS/MS analysis. (**C** and **D**) Examples of the MS/MS spectra of CoA-modified peptides, corresponding to mitochondrial S-type CK 2 (CKMT2) and GAPDH. Proteins identified to be CoAlated in H₂O₂-treated heart (**E**) and liver mitochondria of a 24 h-starved rat (**F**) were grouped into major functional categories. See Supplementary Tables S1 and S2 for

**Figure 4. Proteomic identification of CoAlated proteins in H$_2$O$_2$-treated heart and in the liver of starved rats.** Part 2 of 2 full lists of identified proteins. (**G**) Major metabolic enzymes are CoAlated in H$_2$O$_2$-treated heart (blue circles) and liver mitochondria of a 24 h-starved rat (red circles), ACC, acetyl CoA carboxylase; MCD, malonyl CoA decarboxylase; CPT1, carnitine palmitoyl transferase 1; CACT, carnitine/acylcarnitine carrier protein; DH, dehydrogenase; CS, citrate synthase; IDH, isocitrate dehydrogenase; OGDH, oxoglutarate dehydrogenase; SDH, succinyl-CoA dehydrogenase; MDH, malate dehydrogenase; PDK, pyruvate dehydrogenase kinase; PDH, pyruvate dehydrogenase; GAPDH, glyceraldehyde 3-phosphate dehydrogenase; SCOT, succinyl-CoA: 3-ketoacid CoA transferase; ACAT1, acetyl-CoA acetyltransferase; I–IV, electron transport chain complexes I–IV; Q, coenzyme Q; CytC; cytochrome *C*; F0/F1, ATP synthase; ANT, adenine nucleotide translocase; CK, creatine kinase; BDH1, D-β-hydroxybutyrate dehydrogenase; HMGCL, hydroxymethylglutaryl-CoA lyase; HMGCS2, hydroxymethylglutaryl-CoA synthase; ALDH4A1, Δ-1-pyrroline-5-carboxylate dehydrogenase; ALDH5A1, succinate-semialdehyde dehydrogenase; ALDH6A1, methylmalonate-semialdehyde dehydrogenase [acylating]; ALDH7A1, α-aminoadipic semialdehyde dehydrogenase; Glud1, glutamate dehydrogenase 1; Got2, aspartate aminotransferase; GSTZ1, maleylacetoacetate isomerise; HIBADH, 3-hydroxyisobutyrate dehydrogenase; Kat3, kynurenine–oxoglutarate transaminase 3; PCCA, propionyl-CoA carboxylase. Larger-format versions of panels A-G are available in the Supplementary Material.

protein synthesis, muscle contraction and stress response (Figure 4E,F). A large number of CoAlated proteins are involved in major metabolic pathways, such as the Krebs cycle, β-oxidation, metabolism of glucose, amino acids and ketone bodies, in which CoA and its derivatives are central cofactors and metabolites (Figure 4G). The high prevalence of metabolic enzymes in this analysis is not due to the abundance of these proteins, because similarly abundant ribosomal proteins were not found to be CoAlated (Supplementary Tables S1 and S2).

## CoAlation preferentially targets metabolic enzymes

The susceptibility of metabolic enzymes to CoAlation in response to oxidative and metabolic stress may reflect a potential regulatory or feedback mechanism in which these pathways respond to the CoA/acyl CoA redox state. Therefore, we investigated CoAlation of several enzymes from different metabolic pathways *in vitro* and *in vivo* and examined the effect of this modification on their activities. Initially, we tested whether a set of selected enzymes could be CoAlated *in vitro*. In the present study, recombinant preparations of aconitase 2 (Aco2), HMGCS2, IDH2 and PDK2, as well as CK and GAPDH purified from skeletal muscle, were incubated with or without CoA disulphide (CoASSCoA). Western blot analysis of reaction mixtures with the 1F10 antibody revealed a strong immunoreactive signal corresponding to all tested proteins only in samples incubated with CoA disulphide (Figure 5A). No immunoreactivity was detected in samples separated under reducing conditions (100 mM DTT). Coomassie staining of analysed samples showed that the mobility of Aco2, IDH2, HMGCS2 and PDK2 was retarded when CoA disulphide was present in the reaction mixtures. The addition of DTT completely abolished the observed electrophoretic mobility shifts, indicating the formation of CoA–protein mixed disulphides.

To validate CoAlation of proteins identified by mass spectrometry, we investigated CoAlation of a set of metabolic enzymes in response to oxidative stress in cells. HEK293/Pank1β cells were transiently transfected with plasmids encoding FLAG-tagged forms of CK, GAPDH, IDH2 and PDK2, and then treated with H$_2$O$_2$ or diamide. Immunoprecipitation of transiently expressed FLAG-tagged CK, GAPDH, IDH2 and PDK2 followed by immunoblotting with the 1F10 antibody confirmed that all tested proteins are indeed CoAlated in cells treated with H$_2$O$_2$ or diamide (Figure 5B). Furthermore, CoAlation of several endogenous proteins was examined in heart and liver under various experimental conditions. Immunoprecipitation of endogenous ACAA2 from the liver of control and starved rats revealed starvation-induced CoAlation of ACAA2 (Figure 5C). In contrast, CoAlation of endogenous HMGCS2 was at a high level in the liver of rats kept on a chow diet, but feeding rats a HF/HS diet for 1 week resulted in a substantial decrease in HMGCS2 CoAlation (Figure 5D). ACAA2 and HMGCS2 are key enzymes in β-oxidation and ketogenesis, respectively, so CoAlation of these enzymes may regulate fatty acid oxidation and ketone bodies formation during prolonged starvation or excess supply of nutrients.

Next, we specifically investigated the effect of *in vitro* CoAlation on the activity of CK, GAPDH, IDH2 and PDK2. In the heart, CK is an important source of ATP production and its inactivation is thought to play a critical role in cardiac response to oxidative stress and reperfusion injury [33]. CK is inhibited by GSSG in a
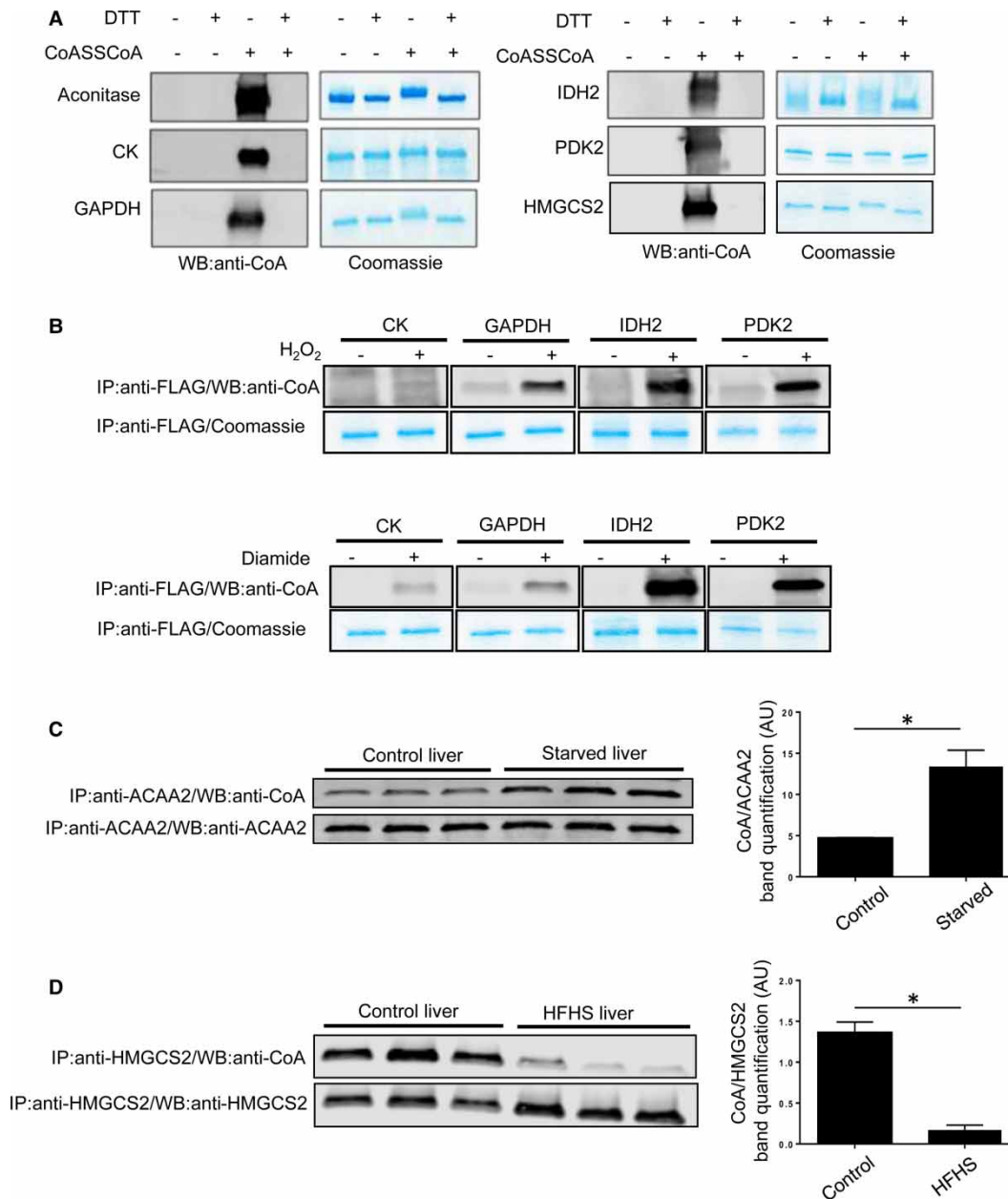
**Figure 5. *In vitro* and *in vivo* CoAlation of metabolic enzymes.**

(**A**) *In vitro* CoAlation of a panel of metabolic enzymes. Recombinant preparations of aconitase, IDH2, PDK2, HMGCS2, as well as CK and GADPH purified from skeletal muscle were incubated with 2–10 mM CoA dimer (CoASSCoA). NEM (25 mM) was added and samples were heated in loading buffer with or without DTT. CoAlation of enzymes was examined by anti-CoA immunoblot. (**B**) FLAG-tagged CK muscle isoform, GAPDH, IDH2 and PDK2 were transiently overexpressed in HEK293/Pank1β. Transfected cells were treated for 30 min with 0.5 mM $H_2O_2$ or 0.5 mM diamide. Overexpressed proteins were immunoprecipitated with an anti-FLAG antibody and immune complexes immunoblotted with anti-CoA antibody. (**C** and **D**) Endogenous ACAA2 and HMGCS2 were immunoprecipitated from the liver of control, 24 h starved rats or rats that were fed HF/HS diet for 1 week and analysed by anti-CoA Western blotting. Data are mean ± SEM of three biological replicates. *$P < 0.05$.

dose-dependent manner [34], with the site of glutathionylation mapped to Cys283. In agreement with this report, we observed full inhibition of CK activity by GSSG which is reversed by DTT (Figure 6A). Notably, the activity of CK was also completely inhibited by incubation with CoASSCoA and the recovery was
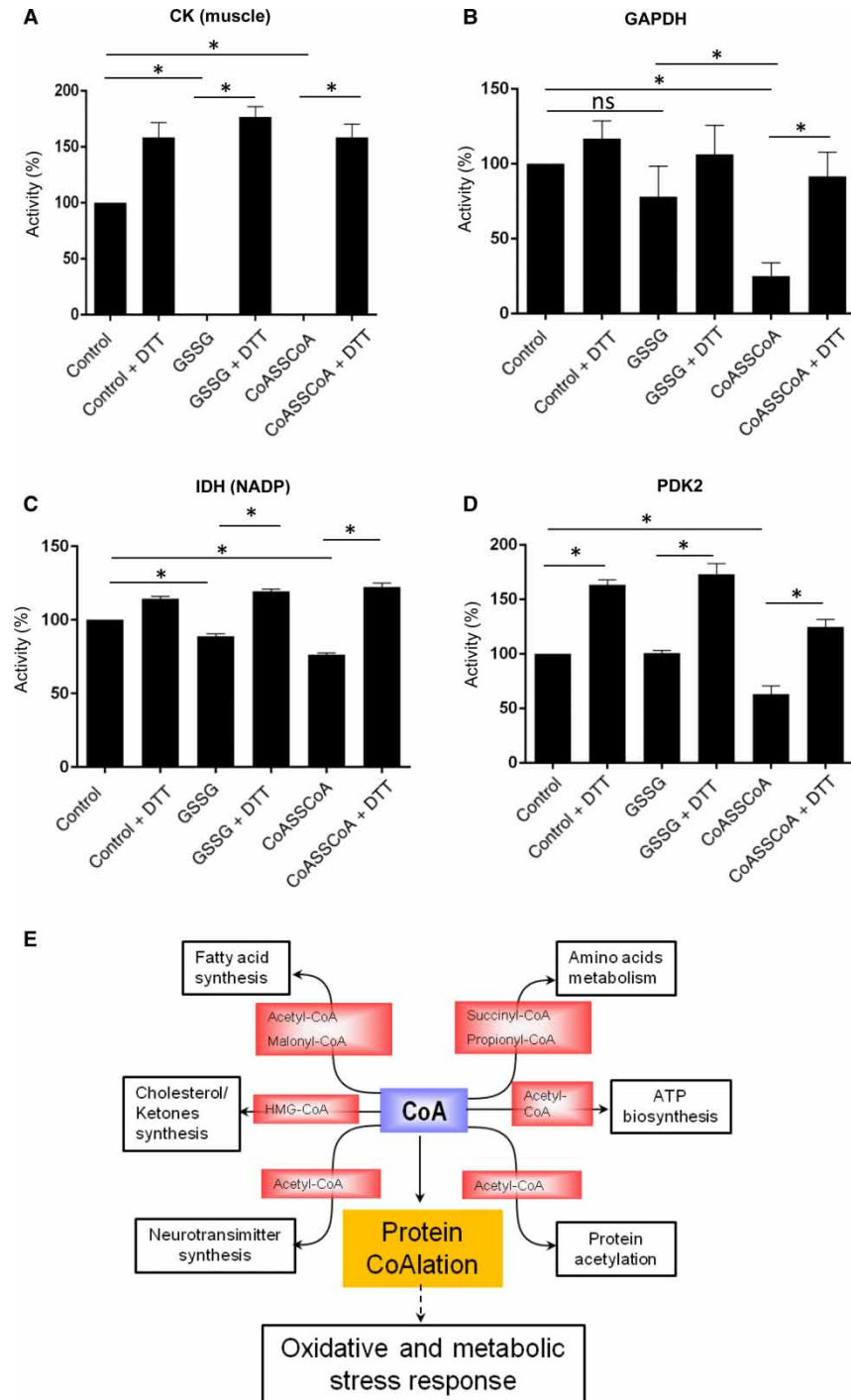
**Figure 6. Catalytic activities of CK, GAPDH, IDH and PDK2 are modulated by CoAlation.**

(**A–D**) CK, GAPDH purified from skeletal muscle and NADP-dependent IDH purified from heart were incubated with CoASSCoA or GSH dimer (GSSG) and their enzymatic activities assayed spectrophotometrically. The activity of recombinant PDK2 purified from HEK293 cells was assayed radiometrically using PDH as the substrate. Data shown are mean ± SEM of 3 (**A**, **C** and **D**) or 5 (**B**) independent measurements. Differences between groups were evaluated by a two-way repeated measures ANOVA matching both factors followed by a Tukey *post hoc* test to correct for multiple comparisons when assessing simple effects or Sidak test when assessing the 'reducing agent' effect. *$P < 0.05$. ns, not significant. (**E**) Cellular functions of CoA. In addition to its well-established role as an essential metabolic cofactor, CoA may also function as an antioxidant in cellular response to oxidative or metabolic stress via protein CoAlation.

DTT-dependent. In $H_2O_2$-treated heart, we identified seven CoAlated peptides corresponding to CKB, CKM, CKMT1 and CKMT2 (Supplementary Table S1), and their role in regulating the function of CK isoforms remains to be elucidated.

GAPDH has a well-established role in glycolysis and is also implicated in the regulation of transcription, initiation of apoptosis and axonal transport [35]. GAPDH possesses a highly conserved catalytic cysteine, which is a target for various thiol modifications, including sulfenylation, glutathionylation and nitrosation. These modifications were shown to modulate its enzymatic activity and regulatory interactions. Here, we show that CoAlation of GAPDH decreases activity *in vitro* by ∼75% and the inhibition is reversed by DTT (Figure 6B). We also found inhibition of GAPDH activity by GSSG, but to a much lesser degree (15%). Cys23 and Cys245 were found to be CoAlated in GAPDH in the heart after $H_2O_2$ treatment. Cys23 is located in close proximity to the NAD-binding pocket, so the modification of this residue by CoA may affect the affinity of interaction with NAD through steric effects. Nitrosation of Cys245 in cellular response to interferon-γ and LDL(ox) was implicated in the formation of the iNOS-S100A8/9 transnitrosylase complex [36]. The relevance of Cys23 and Cys245 CoAlation in the function of GAPDH will be the subject of further studies.

Four CoAlated peptides, corresponding to the mitochondrial NADP-dependent IDH2, were identified in the present study. IDH2 is a key player in intermediary metabolism and energy production, and catalyses the oxidative decarboxylation of isocitrate into α-ketoglutarate in the Krebs cycle [37]. As shown in Figure 6C, the incubation of IDH2 with CoASSCoA significantly reduced its activity, which was restored in the presence of DTT. The role of CoAlated cysteines in the function of IDH2 remains to be investigated although Cys113, Cys418 and Cys308 are located in close proximity to the substrate and NADP-binding sites. It is important to note that the addition of DTT to IDH2, GAPDH, CK and PDK2 increased their activity (Figure 6B–E). This suggests that the enzyme preparations possess reversibly modified cysteine thiols which reduce their enzymatic activities supporting a role in regulation.

PDK2 is an isozyme of PDH kinase which has an active site and an allosteric site co-operating for the activation and regulation of this enzyme. In its active state, PDK2 phosphorylates and inactivates the PDH complex, which is a rate-limiting step in regulating glycolysis and carbohydrate oxidation as well as producing metabolites for oxidative phosphorylation and the electron transport chain [38]. The activity of PDK2 towards PDH has been previously shown to be inhibited by low levels of $H_2O_2$ in heart mitochondria via reversible oxidation of Cys45 and Cys392 [39]. To our knowledge, S-thiolation of PDK2 by low-molecular-weight thiols such as GSH has not been reported. In our study, Cys392 was found to be CoAlated in perfused heart in response to $H_2O_2$ treatment (Supplementary Table S1). As shown in Figure 6D, *in vitro* CoAlation of recombinant PDK2 significantly inhibited its activity and the phosphorylation of PDH was reversed by DTT. Notably, preincubation of PDK2 with oxidised GSSG did not affect its activity towards PDH.

The above findings reveal for the first time that CoA, in addition to its well-established functions in cellular metabolism, may play a major role in the regulation of oxidative and metabolic stress response (Figure 6E).

## Discussion

CoA is at the heart of metabolic integration. CoA generates a diverse range of thioesters which are involved in major metabolic pathways, cholesterol and acetylcholine biosynthesis, and the regulation of gene expression. In the present study, we report a novel function of CoA in the control of cellular redox regulation mediated by reversible covalent modification of various cellular proteins. To be recognised as a redox-control mechanism, protein CoAlation must meet several important criteria, including (a) induction by ROS and/or RNS; (b) reversible modification; (c) modulation of protein activity or function and (d) specificity to regulatory cysteine residues. Here, we provide evidence that protein CoAlation is induced in a dose- and time-dependent manner in mammalian cells treated with different oxidising agents. Secondly, the fast and reversible nature of protein CoAlation is clearly observed when the oxidants are removed from cell cultures. It remains to be elucidated whether the de-CoAlation process is enzymatically driven. Furthermore, protein CoAlation can be effectively blocked by pretreatment of cells with antioxidants. Thirdly, the developed protocol allowed us to identify a wide range of cellular proteins modified by CoA in hearts perfused with $H_2O_2$. A striking feature of redox-regulated protein CoAlation is that it preferentially occurs on proteins involved in metabolic pathways. Finally, a significant difference in the patterns of CoAlated and glutathionylated proteins in $H_2O_2$-treated rat hearts clearly suggests that different regulatory cysteine residues can be specifically targeted by CoA and GSH in response to oxidative stress. To further substantiate these findings, we also demonstrated extensive

oxidant-induced protein CoAlation in prokaryotes, especially in *Staphylococcus aureus*, which produces large quantities of CoA, but lacks detectable levels of GSH (unpublished observation).

What is the relevance of protein CoAlation in the function of mammalian cells? Similarly to glutathionylation, protein CoAlation may function as an important antioxidant defence by preventing the formation of irreversible oxidation of the highly nucleophilic thiol group of cysteine residues located on the surface of cellular proteins. Alternatively, CoAlation can directly regulate the activity of cellular enzymes in response to oxidative or metabolic stress. We also propose that the presence of pantetheine and $3'5'$-ADP moieties on CoA-modified cysteines may generate a unique binding motif for intra- and inter-molecular interactions, especially for proteins containing the Rossmann binding fold.

GSH has been regarded as the main modulator of the redox homeostasis in mammalian cells, and the role of protein glutathionylation in the oxidative stress response has been extensively studied in the last two decades. The present study reveals an alternative mechanism of redox regulation by protein CoAlation and lays a foundation for delineating the role of this post-translational modification under physiological and pathophysiological conditions.

## Abbreviations

4PP, $4'$-phosphopantetheine; ACAA2, 3-ketoacyl-CoA thiolase; Aco2, aconitase 2; BSA, bovine serum albumin; BSA-dpCoA, BSA-dephospho CoA; CK, creatine kinase; CKB, creatine kinase B-type; CKM, creatine kinase M-type; CoA, coenzyme A; CoASSCoA, CoA disulphide; CoASY, CoA synthase; DMEM, Dulbecco's Modified Eagle's Medium; DpCoA, $3'$-dephospho CoA; DTT, dithiothreitol; EDTA, ethylenediaminetetraacetic acid; FBS, foetal bovine serum; GAPDH, glyceraldehyde-3-phosphate dehydrogenase; GSH, glutathione; $H_2O_2$, hydrogen peroxide; HF/HS, high fat/high sucrose; HMGCS2, hydroxymethylglutaryl-CoA synthase 2; IAM, iodoacetamide; IDH2, isocitrate dehydrogenase 2; MeCN, methyl cyanide (aka acetonitrile); NAC, *N*-acetyl-*l*-cysteine; NBIA, Neurodegeneration with Brain Iron Accumulation; NEM, *N*-ethylmaleimide; Nudix7, Nudix hydrolase 7; Ox-LDL, oxidized low-density lipoprotein; Pank, pantothenate kinase; PAGE, polyacrylamide gel electrophoresis; PAO, phenylarsine oxide; PCA, perchloric acid; PDH, pyruvate dehydrogenase; PDK2, pyruvate dehydrogenase kinase 2; PIC, protease inhibitor cocktail; RNS, reactive nitrogen species; ROS, reactive oxygen species; SDS, sodium dodecyl sulphate; TBH, *t*-butylhydroperoxide; TEA, triethanolamine.

## Author Contribution

## Funding

## Acknowledgements

## Competing Interests

The Authors declare that there are no competing interests associated with the manuscript.

PORTLAND
PRESS

# References

1   Leonardi, R., Zhang, Y.-M., Rock, C.O. and Jackowski, S. (2005) Coenzyme A: back in action. *Prog. Lipid Res.* **44**, 125–153 doi:10.1016/j.plipres.2005.04.001

2   Davaapil, H., Tsuchiya, Y. and Gout, I. (2014) Signalling functions of coenzyme A and its derivatives in mammalian cells. *Biochem. Soc. Trans.* **42**, 1056–1062 doi:10.1042/BST20140146

3   Srinivasan, B. and Sibon, O.C.M. (2014) Coenzyme A, more than 'just' a metabolic cofactor. *Biochem. Soc. Trans.* **42**, 1075–1079 doi:10.1042/BST20140125

4   Theodoulou, F.L., Sibon, O.C.M., Jackowski, S. and Gout, I. (2014) Coenzyme A and its derivatives: renaissance of a textbook classic. *Biochem. Soc. Trans.* **42**, 1025–1032 doi:10.1042/BST20140176

5   Robishaw, J.D., Berkich, D. and Neely, J.R. (1982) Rate-limiting step and control of coenzyme A synthesis in cardiac muscle. *J. Biol. Chem.* **257**, 10967–10972 PMID:7107640

6   Tubbs, P.K. and Garland, P.B. (1964) Variations in tissue contents of coenzyme A thio esters and possible metabolic implications. *Biochem. J.* **93**, 550–557 doi:10.1042/bj0930550

7   Smith, C.M., Cano, M.L. and Potyraj, J. (1978) The relationship between metabolic state and total CoA content of rat liver and heart. *J. Nutr.* **108**, 854–862 PMID:641600

8   Smith, C.M. and Savage, Jr, C.R. (1980) Regulation of coenzyme A biosynthesis by glucagon and glucocorticoid in adult rat liver parenchymal cells. *Biochem. J.* **188**, 175–184 doi:10.1042/bj1880175

9   Voltti, H., Savolainen, M.J., Jauhonen, V.P. and Hassinen, I.E. (1979) Clofibrate-induced increase in coenzyme A concentration in rat tissues. *Biochem. J.* **182**, 95–102 doi:10.1042/bj1820095

10  McAllister, R.A., Fixter, L.M. and Campbell, E.H.G. (1988) The effect of tumour growth on liver pantothenate, CoA, and fatty acid synthetase activity in the mouse. *Br. J. Cancer* **57**, 83–86 doi:10.1038/bjc.1988.14

11  Reibel, D.K., Wyse, B.W., Berkich, D.A. and Neely, J.R. (1981) Regulation of coenzyme A synthesis in heart muscle: effects of diabetes and fasting. *Am. J. Physiol.* **240**, H606–H611 PMID:7013504

12  Zhou, B., Westaway, S.K., Levinson, B., Johnson, M.A., Gitschier, J. and Hayflick, S.J. (2001) A novel pantothenate kinase gene (PANK2) is defective in Hallervorden–Spatz syndrome. *Nat. Genet.* **28**, 345–349 doi:10.1038/ng572

13  Dusi, S., Valletta, L., Haack, T.B., Tsuchiya, Y., Venco, P., Pasqualato, S. et al. (2014) Exome sequence reveals mutations in CoA synthase as a cause of neurodegeneration with brain iron accumulation. *Am. J. Hum. Genet.* **94**, 11–22 doi:10.1016/j.ajhg.2013.11.008

14  Jacob, C., Battaglia, E., Burkholz, T., Peng, D., Bagrel, D. and Montenarh, M. (2012) Control of oxidative posttranslational cysteine modifications: from intricate chemistry to widespread biological and medical applications. *Chem. Res. Toxicol.* **25**, 588–604 doi:10.1021/tx200342b

15  Wouters, M.A., Iismaa, S., Fan, S.W. and Haworth, N.L. (2011) Thiol-based redox signalling: rust never sleeps. *Int. J. Biochem. Cell Biol.* **43**, 1079–1085 doi:10.1016/j.biocel.2011.04.002

16  Filipovska, A. and Murphy, M.P. (2006) Overview of protein glutathionylation. *Curr. Protoc. Toxicol.* **26**, 6102 Chapter 6: Unit 6.10 doi:10.1002/0471140856.tx0610s28

17  Grek, C.L., Zhang, J., Manevich, Y., Townsend, D.M. and Tew, K.D. (2013) Causes and consequences of cysteine S-glutathionylation. *J. Biol. Chem.* **288**, 26497–26504 doi:10.1074/jbc.R113.461368

18  Giustarini, D., Rossi, R., Milzani, A., Colombo, R. and Dalle-Donne, I. (2004) S-glutathionylation: from redox regulation of protein functions to human diseases. *J. Cell. Mol. Med.* **8**, 201–212 doi:10.1111/j.1582-4934.2004.tb00275.x

19  Van Laer, K., Hamilton, C.J. and Messens, J. (2013) Low-molecular-weight thiols in thiol-disulfide exchange. *Antioxid. Redox Signal.* **18**, 1642–1653 doi:10.1089/ars.2012.4964

20  Huth, W., Pauli, C. and Möller, U. (1996) Immunochemical detection of CoA-modified mitochondrial matrix proteins. *Biochem. J.* **320**, 451–457 doi:10.1042/bj3200451

21  Lee, J.-W., Soonsanga, S. and Helmann, J.D. (2007) A complex thiolate switch regulates the *Bacillus subtilis* organic peroxide sensor OhrR. *Proc. Natl Acad. Sci. U.S.A.* **104**, 8743–8748 doi:10.1073/pnas.0702081104

22  Kim, J. and Kim, K.-J. (2015) Crystal structure and biochemical properties of ReH16_A1887, the 3-ketoacyl-CoA thiolase from *Ralstonia eutropha* H16. *Biochem. Biophys. Res. Commun.* **459**, 547–552 doi:10.1016/j.bbrc.2015.02.148

23  Schwerdt, G., Möller, U. and Huth, W. (1991) Identification of the CoA-modified forms of mitochondrial acetyl-CoA acetyltransferase and of glutamate dehydrogenase as nearest-neighbour proteins. *Biochem. J.* **280**, 353–357 doi:10.1042/bj2800353

24  Malanchuk, O.M., Panasyuk, G.G., Serbyn, N.M., Gout, I.T. and Filonenko, V.V. (2015) Generation and characterization of monoclonal antibodies specific to Coenzyme A. *Biopolym. Cell* **31**, 187–192 doi:10.7124/bc.0008DF

25  Chouchani, E.T., Pell, V.R., Gaude, E., Aksentijević, D., Sundier, S.Y., Robb, E.L. et al. (2014) Ischaemic accumulation of succinate controls reperfusion injury through mitochondrial ROS. *Nature* **515**, 431–435 doi:10.1038/nature13909

26  Clark, H., Carling, D. and Saggerson, D. (2004) Covalent activation of heart AMP-activated protein kinase in response to physiological concentrations of long-chain fatty acids. *Eur. J. Biochem.* **271**, 2215–2224 doi:10.1111/j.1432-1033.2004.04151.x

27  Tsuchiya, Y., Pham, U., Hu, W., Ohnuma, S.-i and Gout, I. (2014) Changes in acetyl CoA levels during the early embryonic development of *Xenopus laevis*. *PLoS ONE* **9**, e97693 doi:10.1371/journal.pone.0097693

28  Allred, J.B. and Guy, D.G. (1969) Determination of coenzyme A and acetyl CoA in tissue extracts. *Anal. Biochem.* **29**, 293–299 doi:10.1016/0003-2697(69)90312-1

29  Fernández-Vizarra, E., Ferrín, G., Pérez-Martos, A., Fernández-Silva, P., Zeviani, M. and Enríquez, J.A. (2010) Isolation of mitochondria for biogenetical studies: an update. *Mitochondrion* **10**, 253–262 doi:10.1016/j.mito.2009.12.148

30  Cox, J. and Mann, M. (2008) MaxQuant enables high peptide identification rates, individualized p.p.b.-range mass accuracies and proteome-wide protein quantification. *Nat. Biotechnol.* **26**, 1367–1372 doi:10.1038/nbt.1511

31  Rock, C.O., Calder, R.B., Karim, M.A. and Jackowski, S. (2000) Pantothenate kinase regulation of the intracellular concentration of coenzyme A. *J. Biol. Chem.* **275**, 1377–1383 doi:10.1074/jbc.275.2.1377

32    Reilly, S.-J., Tillander, V., Ofman, R., Alexson, S.E.H. and Hunt, M.C. (2008) The nudix hydrolase 7 is an Acyl-CoA diphosphatase involved in regulating peroxisomal coenzyme A homeostasis. *J. Biochem.* **144**, 655–663 doi:10.1093/jb/mvn114

33    Zervou, S., Whittington, H.J., Russell, A.J. and Lygate, C.A. (2016) Augmentation of creatine in the heart. *Mini Rev. Med. Chem.* **16**, 19–28 doi:10.2174/1389557515666150722102151

34    Reddy, S., Jones, A.D., Cross, C.E., Wong, P.S.-Y. and Van Der Vliet, A. (2000) Inactivation of creatine kinase by S-glutathionylation of the active-site cysteine residue. *Biochem. J.* **347**, 821–827 doi:10.1042/bj3470821

35    Nicholls, C., Li, H. and Liu, J.-P. (2012) GAPDH: a common enzyme with uncommon functions. *Clin. Exp. Pharmacol. Physiol.* **39**, 674–679 doi:10.1111/j.1440-1681.2011.05599.x

36    Jia, J., Arif, A., Willard, B., Smith, J.D., Stuehr, D.J., Hazen, S.L. et al. (2012) Protection of extraribosomal RPL13a by GAPDH and dysregulation by S-nitrosylation. *Mol. Cell* **47**, 656–663 doi:10.1016/j.molcel.2012.06.006

37    Raimundo, N., Baysal, B.E. and Shadel, G.S. (2011) Revisiting the TCA cycle: signaling to tumor formation. *Mol. Med.* **17**, 641–649 doi: 10.1016/j.molmed.2011.06.001

38    Roche, T.E. and Hiromasa, Y. (2007) Pyruvate dehydrogenase kinase regulatory mechanisms and inhibition in treating diabetes, heart ischemia, and cancer. *Cell Mol. Life Sci.* **64**, 830–849 doi:10.1007/s00018-007-6380-z

39    Hurd, T.R., Collins, Y., Abakumova, I., Chouchani, E.T., Baranowski, B., Fearnley, I.M. et al. (2012) Inactivation of pyruvate dehydrogenase kinase 2 by mitochondrial reactive oxygen species. *J. Biol. Chem.* **287**, 35153–35160 doi:10.1074/jbc.M112.400002